The Structure of the 2-Norbornyl Cation: The π-Complex and Beyond[†,‡]

Nick H. Werstiuk* and Heidi M. Muchall

Department of Chemistry, McMaster University, Hamilton, Ontario L8S 4M1, Canada

Received: June 21, 1999; In Final Form: December 15, 1999

Calculations at Becke3LYP, MP2, and QCISD levels of theory are presented for different molecular structures of the 2-norbornyl cation (**1**). With the aid of the quantum theory of atoms in molecules (AIM) we show that **1** has a T-structure at the $C^6-C^1-C^2$ face (we view it as a π-complex with a tetracoordinate carbon atom C^6) and that the ("nonclassical") bridged structure with a pentacoordinate C^6, which is not a minimum on the potential energy surface, is only reached when the C^6-C^1 and C^6-C^2 internuclear distances are shortened to 165 pm. At the Becke3LYP/6-31G(d,p) level in the gas phase this bridged species is 7.25 kcal mol^{-1} higher in energy than the equilibrium optimized geometry. NMR calculations show that ^{13}C chemical shifts of C^1, C^2, and C^6 of the bridged 165 pm species differ significantly from the experimental values.

Introduction

A molecule's *structure* (the molecular graph) associated with a given *geometry* (the position of the atoms in space) can be determined unambiguously through an analysis of the electronic charge distribution $\rho(r)$.[3] A bonding interaction between a pair of atoms is indicated by the presence of a (3, −1) critical point (cp) in ρ in the internuclear region, a point where the gradient vector field $\nabla\rho$ is zero and where ρ shows two negative curvatures and one positive.[4] The eigenvector associated with the single positive eigenvalue (curvature) defines a unique pair of trajectories of $\nabla\rho(r)$, originating at the (3, −1) cp and terminating at the nuclei of the pair of atoms, called an atomic interaction line; the eigenvectors associated with the two negative eigenvalues define a set of trajectories terminating at the (3, −1) cp and spanning the interatomic surface shared by the pair of atoms. The atomic interaction line linking the two nuclei is a line through space along which the electronic charge density is a maximum with respect to any neighboring line; for a system at a stationary point it is called a bond path and the (3, −1) critical point a bond critical point (cp_b).[3,5] It is important to understand that "the presence of a bond path provides a universal indicator of bonding between the atoms so connected".[4] No bond path, no bonding.

The network of bond paths for a given geometry is called the molecular graph and changes in the molecular graph can occur when the nuclear configuration is altered. This is illustrated in Figure 1 for a chemical system ABC, with A, B, and C being either atoms or groups of atoms.[3] The two-dimensional cross-section in Figure 1 shows four structural regions in which even considerable changes in geometry do not change the molecular graph and, accordingly, the three chain and one ring structure are said to be stable. The three T-structures located on the boundaries are structurally unstable configurations; they are stable only for the particular (symmetrical) arrangement of the nuclei. A T-structure is generally referred to as a conflict structure, as two attractors (e.g., those of B and C in the topmost molecular graph) are competing for a bond path and a slight asymmetric displacement of a nucleus (i.e., that of A in the above example) causes an abrupt switch of this bond path from one attractor to the other, as shown in Figure 1. This first basic mechanism of structural change is referred to as the conflict mechanism. The second basic mechanism of structural change, the bifurcation mechanism, involves the formation of a degenerate critical point in $\rho(r)$ as found, e.g., in crossing a boundary between chain and ring regions in Figure 1. A trivial change in structure is given by the symmetric displacement of A away from the B−C bond, which will eventually lead to a separation of A and B−C by a simple decay (to zero) of ρ at that (3, −1) critical point.[3]

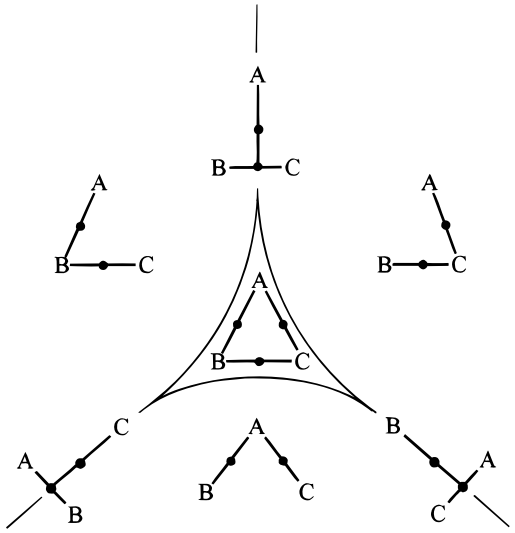

Figure 1. Structure diagram (2-dimensional cross-section) for a chemical system ABC, showing four stable regions: the chains A−B−C, B−C−A, and B−A−C and the three-membered ring. Bond critical points are given as black dots.

The reevaluation of the electronic charge distribution of the 2-norbornyl cation (**1**), which we carried out recently at the Becke3LYP/6-31G(d,p), Becke3LYP/6-311+G(2d,2p), and MP2/6-311G(d,p) levels of theory, revealed that **1** possesses a

[†] Presented at the 82nd CSC conference in Toronto, Ontario, Canada, June 1, 1999.

[‡] While we called the 2-norbornyl cation a π-complex in our earlier communications,[1,2] we use the more descriptive and topologically correct T-structure designation in this paper.

* To whom correspondence may be addressed. Telephone: (905) 525-9140. Fax: (905) 522−2509. E-mail: werstiuk@mcmaster.ca.

10.1021/jp992043b CCC: $19.00
Published on Web 02/23/2000

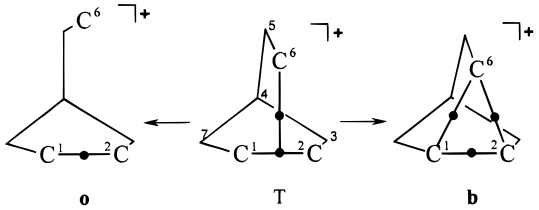

Figure 2. Different structures in the 2-norbornyl cation within C_s symmetry: T, bridged **b**, and open structure **o**.

T-structure (we view it as a π-complex) at the $C^6-C^1-C^2$ face, in which a cation interacts with a double bond and carbon atom C^6 is tetracoordinate.[1] The relevance of the molecular graphs in the ABC system, given in Figure 1, to **1** are immediately obvious. The structure associated with the equilibrium geometry of **1** is represented by one of the unstable configurations in Figure 1 and T in Figure 2 and its conflict nature has been discussed.[1] **1** is not bridged (like the ring structure in Figure 1 and **b** in Figure 2) with corresponding (3, −1) and (3, +1)[4] critical points and a pentacoordinate C^6, as expected in the "nonclassical" picture. While for **1** the T-structure is the global minimum, the structure diagram suggests that the bridged structure should also be accessible, by following the axis down from the topmost configuration. The opposite direction on this axis should lead to yet another change in structure and through it to the open molecular graph **o** (Figure 2) in which C^6 is separated from C^1-C^2, a situation that is different from the simple decay in ρ_b that leads to a separation of A and B−C in the model system.

In this paper, we are employing the quantum theory of atoms in molecules[3] (AIM) to (a) provide further proof that the 2-norbornyl cation (**1**) has a T-structure, (b) establish what it takes to reach the so-called "nonclassical" bridged structure **b**, and (c) determine at what point **1** becomes the open C_s cation **o** by increasing the $C^6-C^1(C^2)$ internuclear distances. Furthermore, we present NMR calculations showing that the ^{13}C shifts of C^1, C^2, and C^6 of the 165 pm geometry which is a bridged species differ significantly from the experimental values.

Computational Details

Becke3LYP,[6] MP2, and QCISD calculations were carried out with Gaussian 94[7] on IBM RS/6000 model 39H, 350, 530, and SP2, CRAY T90, and SGI R10000 Impact computers. The molecules were optimized within C_s symmetry restrictions and with C^6-C^1 and C^6-C^2 distances fixed as indicated in the text. We used the 6-31G(d,p) basis set with Becke3LYP to cover the full range of the C^6-C^1 and C^6-C^2 distances for the analysis of the structural changes in steps ranging from 10 to 20 pm. As outlined in refs 1 and 2, we used this level of theory, because Becke3LYP handles the crucial "classical" 2-norbornyl cation,[8,9] correctly at a reasonably low computational cost[1,2,9] and the inclusion of polarization functions on the hydrogen atoms was essential for the studies performed. When the equilibrium geometry of **1** (a frequency calculation produced all positive eigenvalues and frequencies) was distorted from C_s symmetry and optimized with tight convergence criteria, the C_s-symmetrical species was obtained once more. To check the influence of higher levels of theory on the wave function, some geometries were reoptimized with the 6-311G(d,p) or 6-311+G(2d,2p) basis set. Similarly, selected geometries were optimized with MP2/6-31G(d,p) or MP2/6-311G(d,p) (Tables 1 and 4). Table 4 is available in the Supporting Information. As a final check, QCISD/6-31G(d,p)//MP2/6-31G(d,p) and QCISD/6-31G(d,p)//QCISD/6-31G(d,p) levels were used to obtain the wave function

TABLE 1: Total Energies E_T (au) and Optimized Distances C^6-C^1 and C^6-C^2 $d(C^6-C^{1,2})$ (pm) and C^1-C^2 $d(C^1-C^2)$ (pm) for the C_s-symmetrical 1

	E_T	$d(C^6-C^{1,2})$	$d(C^1-C^2)$
B3LYP/6-31G(d,p)	−273.081485	188.9	139.5
B3LYP/6-31G(d,p)[a]	−273.167891	187.2	139.4
B3LYP/6-31G(d,p)[b]	−273.167754	187.4	139.4
B3LYP/6-311G(d,p)	−273.130701	188.9	139.2
B3LYP/6-311+G(2d,2p)	−273.147579	189.2	138.9
MP2/6-31G(d,p)	−272.221283	182.8	139.4
MP2/6-311G(d,p)	−272.401993	182.8	139.9
QCISD/6-31G(d,p)// MP2/6-31G(d,p)	−272.283127		
QCISD/6-31G(d,p)	−272.283337	184.6	139.1

[a] SCI-PCM$_{mod}$. [b] SCI-PCM$_{def}$.

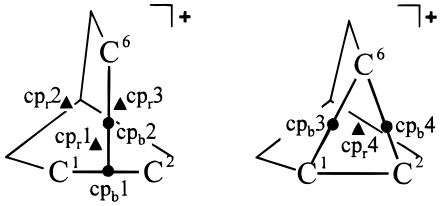

Figure 3. Bond critical points of the $C^6-C^1-C^2$ face and ring critical points in T and bridged structures of **1**.

of the global minimum. The MP2 and QCISD calculations took the correlation effects of all electrons into account. In the beginning, the wave functions obtained at the Becke3LYP level were checked for instabilities; as none were found, MP2 and QCISD wave functions obtained later were not checked but assumed to be stable as well. The total energies reported are uncorrected for zero-point vibrational energies. Given the similarity of the geometrical structures in the crucial region of the potential energy surface, we expected that the inclusion of ZPEs would not alter the relative energies significantly. That this is the case is seen in the fact that the uncorrected and corrected ΔE_T's for optimized **1** and the 165 pm geometrical structure are 7.25 and 7.47 kcal mol^{-1}, respectively. At any rate, whether the corrected or uncorrected energies are used does not impact on the topological analyses.

The studies of the electronic charge density $\rho(r)$, its gradient vector field $\nabla\rho(r)$, and its Laplacian $\nabla^2\rho(r)$ as well as the integrations (to obtain the net charges)[10] were carried out with the AIMPAC[11] series of programs.[12] In the plots of ρ and $\nabla^2\rho$, solid crosses indicate positions of nuclei in the plane and open crosses those of nuclei out of the plane. In the representations of the molecules, the position of a critical point is marked by a dot ((3, −1) cp), a triangle ((3, +1) cp), or a square ((3, +3)[4] cp) (for the numbering of bond and ring cps, see Figure 3). The contour plots of ρ show 40 contour lines between 0.01 and 40.0 au. In the plots of $\nabla^2\rho$, solid lines depict regions of charge concentration, and broken lines those of charge depletion. Ball and cylinder representations are plotted from HyperChem 5.0.[13]

The influence of a solvent on **1** was studied with the self-consistent isodensity polarized continuum model (SCI-PCM)[14] at the Becke3LYP/6-31G(d,p) level. Two types of calculations, SCI-PCM$_{mod}$ and SCI-PCM$_{def}$, were carried out with a dielectric constant of 79.0 (H_2O) at an isodensity value of 0.0004 au and wave functions obtained. For the SCI-PCM$_{mod}$ study involving two geometries (the fully optimized and the 165.0 pm species) the ϕ and θ values for the numerical surface integration using a single origin were set at 72 and 36, respectively, yielding 2596 solvent charges; in the case of the SCI-PCM$_{def}$ calculation, only fully optimized **1** was studied with default values (302 and 1

that define a Lebedev grid are used with the surface integration being piecewise involving the Becke grids), yielding 302 solvent charges.

The isotropic ^{13}C absolute shieldings are calculated for Becke3LYP/6-31G(d,p) geometries at Becke3LYP/6-311+G-(d,p) by employing the continuous set of gauge transformations (CSGT) method of Keith and Bader,[15] as implemented in Gaussian 94. These values are referenced to the ^{13}C absolute shielding of tetramethylsilane calculated at the same level of theory.

Structure of the C_s-Symmetrical 2-Norbornyl Cation

The first topological analysis of the charge density of **1** was presented by Bader in 1985.[16] At the HF/4-21G level of theory, the C_s-symmetrical geometry showed two highly curved bond paths for C^6-C^1 and C^6-C^2, where each integrated path length was 2.46 Å for an internuclear distance of 1.940 Å. The two corresponding (3, −1) critical points were found to be almost on top of each other (the distance between the two was not given) and the (3, +1) cp of the three-membered ring. This structure was reported to be very unstable and easily changed by a coalescence of the ring critical point with a bond critical point of one of the bridging bonds. But at the level of theory applied, the C_s-symmetrical geometry was found to be 0.2 kcal mol^{-1} higher in energy than the fully optimized geometry (of C_1 symmetry, the "classical" cation), which indicates that the computational level was not adequate. The problem of finding the right computational level for the description of the 2-norbornyl cation was addressed recently in computational studies by Schleyer et al.,[8] who found that, with MP2(full)/6-31G(d), the "classical" 2-norbornyl cation is a transition state in the rearrangement from the 2-norpinyl cation to the C_s-symmetrical 2-norbornyl cation whereas it is not a stationary point at the HF/6-31G(d) level. Not surprisingly, the computationally inexpensive HF-DFT hybrid theory Becke3LYP was found to describe the 2-norbornyl cation adequately as well.[1,2,9]

At the Becke3LYP/6-31G(d,p) level,[1] the C^1-C^2 bond length is 139.5 pm, which is that of a partial double bond (the C−C bond length in benzene is calculated at 139.7 pm). The C^6-C^1 and C^6-C^2 distances are enlarged to 188.9 pm, an interatomic separation that goes way beyond what is normal for a C−C single bond. In accord with this, the topological analysis of the charge density for this geometry of **1** reveals that $\rho(r)$ is consistent only with a T-structure. There are only two (3, −1) critical points with their corresponding bond paths on the $C^6-C^1-C^2$ face. The first bond path connects C^1 and C^2 and has the bond critical point cp_b1; the large value of ρ, the large negative value of $\nabla^2\rho$, and the greater than zero ellipticity ϵ[17] at cp_b1 (entry "opt" given in Table 2) are those of a typical partial double bond and, interestingly, are close to the values for the bond critical point of a C−C bond in benzene at the same computational level (ρ 2.103 e $Å^{-3}$, $\nabla^2\rho$ −20.46 e $Å^{-5}$, ϵ 0.21). The second bond path connects C^6 to cp_b1 and has the bond critical point cp_b2. This nontransversal intersection of the bond path of one (3, −1) cp with the interatomic surface of another (3, −1) cp (the T-form) is a characteristic of relatively large interatomic separations that are associated with a weak interaction.[3] Accordingly, ρ at cp_b2 is small and its Laplacian is positive (Table 2), indicating that the accumulation of charge density toward the bond path (the two negative curvatures λ_1 and λ_2) is dominated by the expansion of charge density along the bond path (the one positive curvature λ_3). The conflict nature of the T-structure is reflected in the high ellipticity of 7.97 at cp_b2; the major axis (the axis of λ_2) lies parallel to the C^1-C^2 bond. The contour plots of ρ for the $C^6-C^1-C^2$ (with C^6 at the top) and the symmetry plane, with bond paths as well as interatomic surfaces due to cp_b1 and cp_b2 superposed, are given in Figure 4a,b, respectively. Cp_b2 (see Figure 3) is a saddle point in ρ in these two planes, the trajectories of the interatomic surfaces originating either at infinity or at the (3, +3) critical point (which can only appear as a minimum in ρ). While cp_b1 is a saddle point in Figure 4a, it is a maximum in the plane that is perpendicular to the C−C partial double bond and bisects it (Figure 4b). The saddle feature just below the minimum of the (3, +3) cp in Figure 4b arises from the (3, +1) cp of the five-membered ring at the base of the molecule in this orientation (cp_r1). Finally, the plot of $\nabla^2\rho$ for the $C^6-C^1-C^2$ plane obtained from the wave function calculated at the Becke3LYP/6-31G-(d,p) level is shown in Figure 4c. From this plot it is seen that the valence shell of C^6 exhibits only one maximum in the direction of the partial double bond between C^1 and C^2 (it is pointed out by the arrow); two maxima would be expected for a bridged, pentacoordinate species, as will be demonstrated below. In all, C^6 exhibits four valence shell charge concentrations (VSCCs), as given in Figure 5a (the one pointed toward the C^1-C^2 bond and one each associated with the C^6-C^5 and the two C−H bonds) and is therefore tetracoordinate, not pentacoordinate, as has been suggested.[18,19]

This structure of the global minimum of **1**, originating in the charge density and described by its topology as in the discussion above, was obtained at all higher levels of theory applied. The MP2 method predicts geometries with shorter C^6-C^1 and C^6-C^2 distances, those from the QCISD optimization lie between MP2 and Becke3LYP (Table 1). The data from MP2 and QCISD wave functions regarding $\rho(r)$ correlate with the results from the Becke3LYP calculations and are collected in Table 3 that is available in the Supporting Information. Figure 4d shows $\nabla^2\rho$-(r) at MP2/6-311G(d,p) with C^6-C^1 and C^6-C^2 distances at 182.8 pm. The differences between parts c and d of Figure 4 are not qualitative (the valence shell of C^6 still exhibits only

TABLE 2: Bond Critical Point (cp_b) Data for Different C_s-Symmetrical Geometries of 1 (Becke3LYP/6-31G(d,p)) [ρ (e $Å^{-3}$), $\nabla^2\rho$ (e $Å^{-5}$), and ϵ, as Well as λ_1, λ_2, and λ_3 (e $Å^{-5}$)]

geometry	cp_b	ρ	$\nabla^2\rho$	ϵ	λ_1	λ_2	λ_3
			In the Gas Phase				
155 pm	cp_b1	2.062	−18.63	0.24	−14.89	−12.03	8.29
	cp_b3[a]	1.415	−3.37	4.49	−9.13	−1.66	7.42
165 pm	cp_b1	2.093	−19.79	0.17	−15.18	−12.94	8.31
	cp_b3[a]	1.184	−0.79	27.14	−7.37	−0.27	6.84
170 pm	cp_b1	2.107	−20.22	0.16	−15.30	−13.23	8.31
	cp_b2	1.084	−0.17	55.18	−6.60	−0.12	6.55
opt	cp_b1	2.139	−21.04	0.14	−15.64	−13.69	8.29
	cp_b2	0.762	1.01	7.97	−4.17	−0.46	5.64
	cp_b (C^5-C^4)[b]	1.620	−12.72	0.01			
280 pm	cp_b1	2.226	−22.46	0.23	−16.65	−13.57	7.76
	cp_b2	0.139	0.84	1.48	−0.39	−0.14	1.37
	cp_b (C^5-C^4)[b]	1.289	−7.98	0.01			
320 pm	cp_b1	2.267	−23.04	0.28	−17.11	−13.35	7.42
	cp_b (C^5-C^4)[b]	1.080	−5.28	0.01			
			In Solvent				
165 pm	cp_b1	2.095[c]	−19.81	0.18			
	cp_b3[a]	1.185[c]	−0.84	23.86			
opt	cp_b1	2.142 (2.144)[d]	−21.11 (−21.13)	0.14 (0.14)			
	cp_b2	0.788 (0.786)[d]	0.92 (0.92)	8.41 (8.29)			

[a] Data apply to cp_b4 as well. [b] The C^5-C^4 geometric bond distances for the optimized, 280, and 320 pm geometries are 154.5, 162.5, and 169.2 pm, respectively. [c] For SCI-PCM_{mod}. [d] The first value is for SCI-PCM_{mod}, and the second value is for SCI-PCM_{def}.

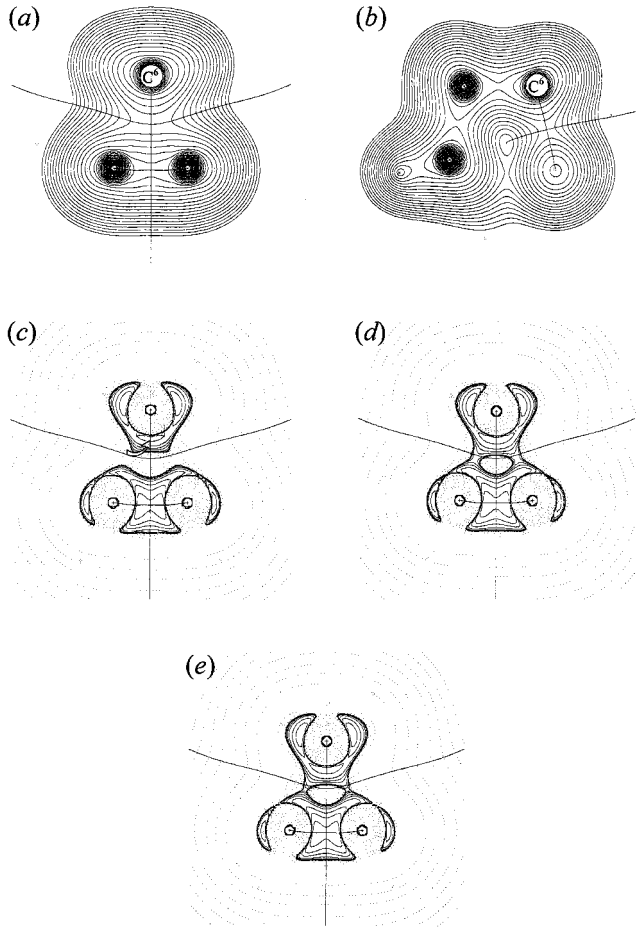

Figure 4. Displays of (a) $\rho(r)$ in the $C^6-C^1-C^2$ plane, (b) $\rho(r)$ in the symmetry plane, and (c)−(e) $\nabla^2\rho(r)$ in the $C^6-C^1-C^2$ plane. (a)−(c) are Becke3LYP/6-31G(d,p) results, (d) is MP2(full)/6-311G(d,p), and (e) is QCISD(full)/6-31G(d,p). Bond paths and interatomic surfaces are superposed on the plots. The arrow in (c) points to the one maximum in the valence shell of C^6 in this plane.

one maximum pointed at the C^1-C^2 bond in Figure 4d) but arise from a simple change in phase of the close-to-zero $\nabla^2\rho$ values at the C^6 interatomic surface between C^6 and C^1 as well as C^6 and C^2. $\nabla^2\rho(r)$ at the QCISD/6-31G(d,p) level resembles that obtained from MP2 calculations closely and is shown for the $C^6-C^1-C^2$ plane in Figure 4e.

Bridged Structure

According to the structure diagram given in Figure 1, bringing A closer to the B−C bond should eventually lead to a bifurcation point and to the formation of a three-membered ring. This is indeed the case when C^6-C^1 and C^6-C^2 distances in the 2-norbornyl cation are shortened within C_s symmetry restrictions. At the Becke3LYP/6-31G(d,p) level, from 188.9 pm in the optimized geometry to 170 pm, the structure does not change and the T-form persists. But shortening the distance to 165 pm finally gives the bridged structure, less stable than the minimum by 7.25 kcal mol^{-1}, that (wrongly) has been assigned to **1** for 50 years. This change in structure and its implication for ^{13}C NMR of the 2-norbornyl cation is explained in detail in the following paragraphs. Total energies for the 155, 165, 170, 280, and 320 pm geometrical sturctures are given in Table 4 that is available as Supporting Information.

A shortening of the C^6-C^1 and C^6-C^2 distances causes the ellipticity for cp_b2 to increase dramatically, an indication that the system approaches the bifurcation point. The increase in ϵ at cp_b2 from 7.97 in the optimized geometry to 55.18 at 170 pm, the largest ellipticity observed in the system, is a result of changes in λ_1 and λ_2 working together. An increasing contraction of density toward the bond path, i.e., a more negative λ_1, can be seen in Table 2. Because the change in the soft curvature λ_2 is enhancing ϵ, it is working against this contraction, but it is less pronounced. The overall effect is a larger ρ and a (slightly) negative $\nabla^2\rho$ at cp_b2 at 170 pm. At 165 pm, a point just past the bifurcation, the cp_bs of the two bridging bonds, cp_b3 and cp_b4 (we reserve cp_b2 for the T-structure; see Figure 3), and the newly formed ring critical point cp_r4 are very close together, the separation between cp_r4 and each of the cp_bs is only 9.8 pm. Accordingly, the two bond paths, C^6-C^1 and C^6-C^2, are highly curved inward and the length of each (194.8 pm) exceeds the geometrical distance by about 30 pm (Figure 6a). λ_2 at cp_b3 and cp_b4 at 165 pm has reversed its trend and is now following that of λ_1 (there is a contraction of charge density along the eigenvectors associated with λ_1 and λ_2) and as a result ϵ is decreased and ρ and $-\nabla^2\rho$ keep growing in magnitude. Because of the proximity of the three critical points, the values for ρ at cp_b3, cp_b4, and cp_r4 (1.184 e $Å^{-3}$) are identical, a typical situation for a three-membered ring, where the three are usually close in value.[3] The plot of $\nabla^2\rho$ for the $C^6-C^1-C^2$ plane with superposed bond paths and interatomic surfaces is shown in

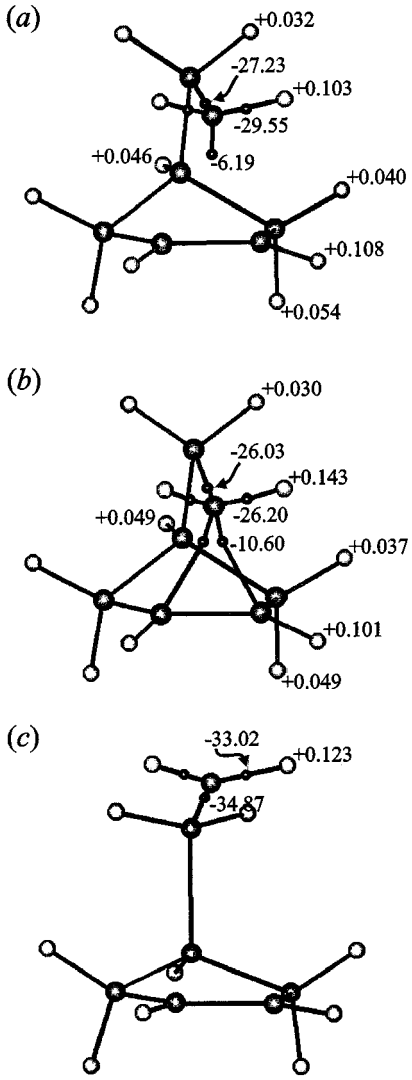

Figure 5. Values of $\nabla^2\rho$ (e $Å^{-5}$) for the valence shell maxima of C^6 (given as small black spheres) and net charges on hydrogen atoms for (a) optimized, (b) 165 pm, and (c) 320 pm geometries of **1**.

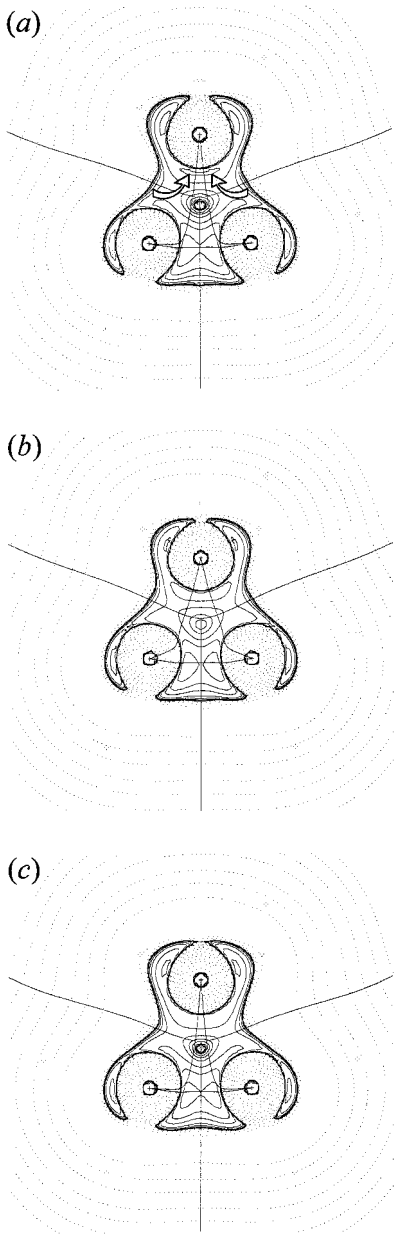

Figure 6. Plots of $\nabla^2\rho(r)$ for the $C^6-C^1-C^2$ plane of **1** with bond paths and interatomic surfaces superposed: for the (a) 165 and (b) 155 pm geometry with Becke3LYP/6-31G(d,p) and (c) for the 165 pm geometry with MP2(full)/6-311G(d,p). The arrows in (a) point to the maxima in the valence shell of C^6 in this plane.

Figure 6a and the difference to the plots in Figure 4 is immediately obvious. Unlike in the T-structure, the valence shell of C^6 in the 165 pm geometry exhibits two maxima in the general direction of the C^1-C^2 bond, one is pointed at C^1, the other at C^2 (both are marked by arrows). In all, C^6 possesses five VSCCs as given in Figure 5b, which makes it a truly pentacoordinate, bridged carbon atom.

Cp_b3 and cp_b4 move further outward and away from cp_r4 (the distance between cp_r4 and each of the cp_bs grows to 22.8 pm) as the C^6-C^1 and C^6-C^2 distances are shortened to 155 pm and the respective bond paths are less curved (the total length of each is 165.7 pm); the system is now destabilized by 17.96 kcal mol^{-1}. ρ at cp_b3 and cp_b4 has almost reached the value of a C−C single bond (1.615 e $Å^{-3}$ in cyclopropane) and, in accord with this, so have λ_1 and λ_3 (λ_1 −10.94, λ_2 −7.45, λ_3 7.95 e $Å^{-5}$ in cyclopropane). The absolute value of λ_2, on the other hand, is still small, which accounts for the high ellipticity and the small negative Laplacian of cp_b3 and cp_b4 (ϵ 0.47, $\nabla^2\rho$ −10.43 e $Å^{-5}$ in cyclopropane). Remarkably, the remaining third bond (C^1-C^2) of the three-membered ring resists change and exhibits an internuclear distance of 140.2 pm; it remains a partial double bond, but all characteristic values are slowly moving away from those of benzene (λ_1 −15.64, λ_2 −12.89, λ_3 8.07 e $Å^{-5}$ for a C−C cp_b in benzene). The Laplacian of ρ at the 155 pm geometry is given in Figure 6b, which illustrates nicely how electronic charge is delocalized over the face of the $C^6-C^1-C^2$ ring.[3] A comparison of Figure 6a,b in terms of the two valence shell charge concentrations on C^6 that are pointed at C^1 and C^2 shows their growth as the nuclei approach each other.

This result, the change in structure upon compression of the system, was obtained with a bigger basis set (6-311G(d,p)) as well as at the MP2 levels. In all cases checked, the 165 pm geometry is bridged while ρ at 170 pm still shows the T-structure. The destabilization (Table 4) for the 165 pm geometry at the two MP2 levels is about 4.9 kcal mol^{-1}, which indicates that these MP2 geometries are closer to the bifurcation point than the Becke3LYP geometry described above. This is in line with the optimized C^6-C^1 and C^6-C^2 distances at MP2 (which are slightly shorter than with Becke3LYP (Table 1)), the distance between cp_r4 and cp_b3 (and cp_b4) of 7.8 pm, and the slightly longer C^6-C^1 and C^6-C^2 bond paths (the total bond path length for each is 197.1 pm at MP2(full)/6-311G(d,p)). The good agreement between the different levels of theory is also evident when the Laplacian of the 165 pm geometry (obtained with MP2(full)/6-311G(d,p) and given in Figure 6c) is compared to that from the lower level of theory (Figure 6a).

The pentacoordinate carbon atom in the bridged structure can only be realized if the fifth bond is formed at the cost of the three that are present in both structures, two C−H and one C^6-C^5 bond. While this can be seen in the decreasing values of ρ and $-\nabla^2\rho$ at the respective bond critical points (data not given), the effect is best evaluated by a comparison of the magnitude of the Laplacian at the positions of the maxima in the valence shell of C^6, which are given in Figure 5 as small black spheres. In the optimized geometry, where C^6 is tetracoordinate (Figure 5a), $-\nabla^2\rho$ is largest in the direction of the two C−H bonds and fairly small in the direction of the partial double bond. In the 165 pm geometry, with a pentacoordinate C^6 (Figure 5b), $-\nabla^2\rho$ at the two newly formed maxima has grown substantially. While it is decreased at the other three maxima, the two C−H bonds are affected more than the C^6-C^5 bond. This in turn is in agreement with the change of the net charge on the hydrogen atoms of these C−H bonds as depicted in Figures5 and 7. While the positive charge is distributed over all of the hydrogen atoms (as was published earlier),[16] the distribution is not even. Figure 5 shows that the biggest contribution is due to the H atoms on C^1, C^2, and C^6, whereas in the neutral norbornane all H atoms bear a similar charge of −0.04 at the Becke3LYP/6-31G(d,p) level. The most prominent change (compare charges in Figure 5a,b) occurs on the C^6 H atoms: the 11 H atoms carry 71% of the total positive charge in the optimized geometry, which is increased to 76% at 165 pm, and most of this additional charge ends up on the C^6 H atoms (the change in charge for these atoms is depicted in Figure 7). This then seems to be the important requirement for a bridged 2-norbornyl cation: in order for C^6 to be pentacoordinate, the cation needs to push positive charge out onto the substituents connected to C^6. That this is indeed the necessary criterion for engineering a bridged 2-norbornyl cation will be shown in a following paper.[20]

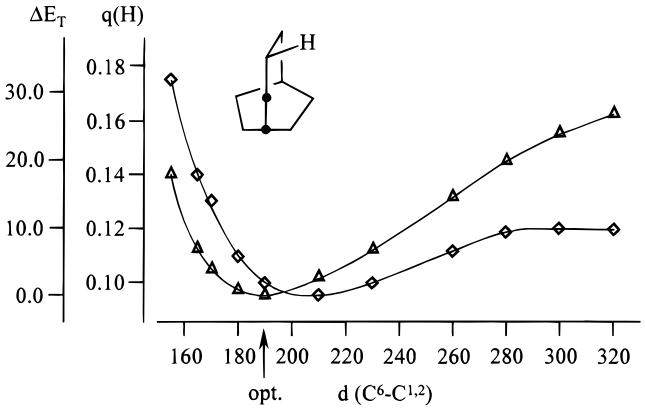

Figure 7. Plots of the relative energies ΔE_T (symbol Δ, kcal mol^{-1}) and the net charges on the C^6 H atoms $q(H)$ (symbol $\diamond$) for different C^6-C^1 and C^6-C^2 distances $d(C^6-C^{1,2})$ (pm) of **1** (Becke3LYP/6-31G(d,p)).

TABLE 5: Computed[a] (for Fully Optimized, 165 pm, and 182.8 pm geometries of 1, Becke3LYP/6-311+G(d,p)// Becke3LYP/6-31G(d,p)) and Experimental ^{13}C Chemical Shifts δ (ppm)

		δ for C at position				
		1, 2	3, 7	4	5	6
opt	^{13}C	137.10	41.38	47.28	23.04	37.68
182.8 pm	^{13}C	128.55	41.09	44.29	23.42	23.82
165 pm	^{13}C	96.81	41.03	36.62	27.00	−8.31
exp[b,c]	^{13}C	124.5	36.3	37.7	20.4	21.2

[a] Referenced to TMS; the calculated absolute shielding of TMS at the Becke3LYP/6-311+G(d,p) level is 181.98 for carbon; the experimental value for carbon is 188.1.[23] [b] At 115 K. [c] At 114 K.

We now compare the computed ^{13}C NMR chemical shifts of the T-species and 165 pm species with the experimental values.[21,22] The chemical shifts of carbon atoms 3, 4, 5, and 7 vary only slightly in going from optimized **1** to the 165 pm geometry. In contrast to this, the chemical shifts of carbon atoms 1, 2, and 6 change by more than 40 ppm (upfield). Also included are the results for the 182.8 pm geometry (these C^6-C^1 and C^6-C^2 distances correspond to those found for the optimized geometry at the MP2 levels, the shortest distances encountered in our full optimizations (Table 1)) calculated with Becke3LYP/6-31G(d,p). This geometry gives chemical shifts that are improved over those for the optimized geometry even though they are uniformly too high by an average 4.3 ppm. This indicates that the C^6-C^1 and C^6-C^2 distances are probably closer to 182.8 pm (the MP2 value) than to the computed, fully optimized value of 188.9 pm (Becke3LYP), which is supported by the QCISD distance of 184.6 pm. Contrary to what was stated before,[18,21] the observed shifts of 124.5 ppm for C^1 and C^2 and 6.75 ppm for their hydrogen nuclei are again those for a partial double bond (as observed, e.g., in *p*-xylene, 134.5 and 6.97 ppm, and 1,3-butadiene, 137.1 and 6.27 ppm) and bridging is expressed in much more shielded carbon nuclei 1, 2, and 6. For the 165 pm geometry where bridging is first manifested, C^6 is predicted to exhibit a chemical shift of −8.3 ppm! Likewise, C^1 and C^2, which are now tetracoordinate, are moving out of the high field end of the doubly bonded region; the data for a bridged, pentacoordinate C^6 do *not* agree with the observed chemical shifts.

Open Structure

In the structure diagram in Figure 1, a symmetric displacement of A away from the B−C bond will eventually lead to a separation of A and B−C by a simple decay (to zero) of ρ at that (3, −1) critical point.[3] For the formation of the open molecular graph **o** (Figure 2) in which C^6 is separated from C^1-C^2, cp_b2 in the 2-norbornyl cation cannot vanish in a similar fashion, as two ring cps and one cage cp have to disappear as well.

The cage structure of the T-form persists up to C^6-C^1 and C^6-C^2 distances of 280 pm (Becke3LYP/6-31G(d,p)), where cp_r2, cp_r3, and the cage cp are on the verge of merging, the cage cp is separated from each of the two ring cps by only 5.2 pm (38.3 pm in the optimized geometry), and ρ with 0.109 e Å^{-3} is the same for all three cps. These three cps have moved toward cp_b2, closing the distance between it and the cage cp to 57.3 pm from an initial 89.3 pm. ρ at cp_b2 has decreased substantially (Table 2) and is close to that of the three approaching cps. Somewhere between 280 and 300 pm, the two ring and one cage cp merge to form a singularity in ρ and at 300 pm this has transformed into a new (3, +1) cp, separated from cp_b2 by only 41.8 pm. The cage structure is lost and while the five-membered ring at the base of the molecule is still present, C^1, C^2, C^3, and C^7 are no longer considered to be part of a ring containing C^5 and C^6. Because of the proximity of the ring cp and cp_b2, this structure again is very unstable and the newly formed ring cp (0.089 e Å^{-3}) and cp_b2 are close to merging. Finally, at 320 pm, 27.25 kcal mol^{-1} above the minimum geometry, these two cps have annihilated each other and the T-form has vanished (yet ρ at the now (2, 0) cp is still a substantial 0.06 e Å^{-3}). The partial double bond of the energy minimum has turned into essentially a full double bond with a geometrical bond length of 135.8 pm (the C−C bond length in ethene is calculated at 133.0 pm); cp_b1 in this open structure reflects this with ρ 2.267 e Å^{-3}, $\nabla^2\rho$ −23.04 e Å^{-5}, and ϵ 0.28 (the values for ethene at this level of theory are ρ 2.345 e Å^{-3}, $\nabla^2\rho$ −24.62 e Å^{-5}, and ϵ 0.39). In accord with the C^1-C^2 double bond, C^6 is tricoordinate. Figure 5c shows the positions of the three maxima in the valence shell of C^6, the value of $\nabla^2\rho$ at these points, and the charge on the hydrogen atoms on C^6. Unlike the bridged cation, which has to weaken both C−H bonds as well as the C^6-C^5 bond in order to become pentacoordinate, the open primary cation strengthens all three bonds: as C^6 is displaced away from C^1-C^2 and the C_s geometry is maintained, there is an increased hyperconjugation interaction with the C^5-C^4 bond, as evidenced by the increase in the geometric bond length and in the change in the properties of the C^5-C^4 cp_b with ρ and $\nabla^2\rho$ decreasing to 1.080 e Å^{-3} and −5.28 e Å^{-5}, respectively (Table 2). This, of course, is normal chemical behavior and implies that it should be possible to move toward an open C_s species by placing substituents on C^6 that are capable of stabilizing a primary cation by hyperconjugation. Examples of systems engineered in this fashion will be given in a following paper.[20]

Effect of Solvent on the Structure and Energetics of the 2-Norbornyl Cation

To probe the effect of solvent on the geometry, structure, and energetics of **1**, calculations were carried out with the self-consistent isodensity polarized continuum model (SCI-PCM) at the Becke3LYP/6-31G(d,p) level. The SCI-PCM procedure solves for the electron density which minimizes the energy including the solvation energy.[14] The effects of solvent are included in the iterative SCF calculation, which accounts for the full coupling between an optimized cavity and the electron density. With the SCI-PCM_{mod} setup (see computational details), the C^6-C^1 (and C^6-C^2) and C^1-C^2 interatomic distances for

fully optimized **1** are 187.2 and 139.4 pm, respectively, and the cation is stabilized by 54.22 kcal mol^{-1} relative to the gas-phase species (Table 1). With the SCI-PCM_{def} setup, these interatomic distances are 187.4 and 139.4 pm, respectively, and the cation is stabilized by 54.13 kcal mol^{-1}; the default SCI-PCM parameters adequately recover the solvation energy of **1**. In both cases the T-structure is retained and the data for cp_b1 and cp_b2 vary only slightly from those obtained in the gas phase as expected for the similar geometries (Table 2).

When SCI-PCM_{mod} is employed, the 165 pm species is 6.47 kcal mol^{-1} (for the gas-phase species the difference is 7.25 kcal mol^{-1}) higher in energy than the fully optimized, solvated cation (Tables 1 and 4), which is in accord with the shorter distance in the latter as compared to the fully optimized **1** in the gas phase. Three (3, −1) cps and a (3, +1) cp are found for the $C^6-C^1-C^2$ face, virtually in the same locations as in the gas phase species, indicating that the solvated cation is also slightly beyond the bifurcation point. Accordingly, the critical point data for cp_b1, cp_b3, and cp_b4 are very similar to those for the gas phase 165 pm geometry (Table 2). These results indicate that solvation of the 2-norbornyl cation by a polar solvent changes the geometry marginally but does not alter its structure.

Conclusion

The topology of the charge density of the 2-norbornyl cation (**1**) is that of a T-form, with C^6 being tetracoordinate, and not that of a pentacoordinate, bridged species. The bridged cation, which is not a minimum on the potential energy surface, has been characterized for the first time and it has been shown that, upon bridging, **1** pushes out more positive charge onto the hydrogen atoms on C^6 and weakens the corresponding C−H bonds. If this is taken into consideration, it will be possible to engineer truly bridged 2-norbornyl cations through the right choice of substituents. Similar considerations should make it possible to engineer C_s carbocations that move toward the open geometry.

Acknowledgment. We gratefully acknowledge the grant of CPU time on a CRAY T90 vector computer in the NIC at the Research Center Jülich, the usage of the IBM SP2 computer at Queen's University granted under the auspices of an IBM Canada−Queen's University collaborative project as well as the usage of the SGI computing installation in the Geochemistry Labs at McMaster funded by NSERC. We thank the Natural Sciences and Engineering Research Council of Canada for financial support.

Supporting Information Available: Tables 3 and 4 containing bond critical point data and total energies. This information is available free of charge via the Internet at http://pubs.acs.org.

References and Notes

(1) Werstiuk, N. H.; Muchall, H. M. *THEOCHEM* **1999**, *463*, 225.
(2) Muchall, H. M.; Werstiuk, N. H. *Can. J. Chem.* **1998**, *76*, 1926.
(3) Bader, R. F. W. *Atoms in Molecules. A Quantum Theory*; Clarendon Press: Oxford, U.K., 1990.
(4) A critical point is labeled by giving the rank ω, the number of nonzero curvatures of ρ, and the signature σ, the algebraic sum of the signs of the curvatures of ρ, as (ω, σ).[3] A (3, +1) or ring critical point possesses two positive and one negative curvature, and at a (3, +3) or cage critical point all three curvatures are positive.
(5) Bader, R. F. W. *J. Phys. Chem. A* **1998**, *102*, 7314.
(6) Becke, A. D. *J. Chem. Phys.* **1993**, *98*, 5648. Lee, C.; Yang, W.; Parr, R. G. *Phys. Rev. B* **1988**, *37*, 785.
(7) Frisch, M. J.; Trucks, G. W.; Schlegel, H. B.; Gill, P. M. W.; Johnson, B. G.; Robb, M. A.; Cheeseman, J. R.; Keith, T.; Petersson, G. A.; Montgomery, J. A.; Raghavachari, K.; Al-Laham, M. A.; Zakrzewski, V. G.; Ortiz, J. V.; Foresman, J. B.; Peng, C. Y.; Ayala, P. Y.; Chen, W.; Wong, M. W.; Andres, J. L.; Replogle, E. S.; Gomperts, R.; Martin, R. L.; Fox, D. J.; Binkley, J. S.; Defrees, D. J.; Baker, J.; Stewart, J. P.; Head-Gordon, M.; Gonzalez, C.; Pople, J. A. *Gaussian 94*, Revision B.3; Gaussian, Inc.: Pittsburgh, PA, 1995.
(8) (a) Sieber, S.; Schleyer, P. v. R.; Vancik, H.; Mesic, M.; Sunko, D. E. *Angew. Chem., Int. Ed. Engl.* **1993**, *32*, 1604. (b) Schleyer, P. v. R.; Sieber, S. *Angew. Chem., Int. Ed. Engl.* **1993**, *32*, 1606.
(9) Schreiner, P. R.; Schleyer, P. v. R.; Schaefer, H. F., III. *J. Org. Chem.* **1997**, *62*, 4216.
(10) The net charge on an atom is calculated by integrating the charge density over the atomic basin and subtracting the so obtained number of electrons from the nuclear charge.
(11) Biegler-König, F. W.; Bader, R. F. W.; Tang, T.-H. *J. Comput. Chem.* **1982**, *3*, 317.
(12) Available from Professor R. F. W. Bader, McMaster University, Hamilton, ON L8S 4M1, Canada, and from the AIMPAC website (www.chemistry.mcmaster.ca/aimpac).
(13) *HyperChem 5.0*; Hypercube Inc.: Waterloo, ON N2L 3X2, Canada.
(14) Foresman, J. B.; Frisch, A. E. *Exploring chemistry with electronic structure methods*, 2nd ed.; Gaussian Inc.: Pittsburgh, PA, 1996.
(15) Keith, T. A.; Bader, R. F. W. *Chem. Phys. Lett.* **1992**, *194*, 1. Keith, T. A.; Bader, R. F. W. *Chem. Phys. Lett.* **1993**, *210*, 223.
(16) Bader, R. F. W. *Acc. Chem. Res.* **1985**, *18*, 9.
(17) Along a bond path, the charge density is a minimum at a (3, −1) critical point and the corresponding curvature (or eigenvalue of the Hessian of ρ) λ_3 is positive. Both λ_1 and λ_2 are negative, with λ_2 being of the smaller magnitude, the ellipticity ϵ at the (3, −1) cp is determined as $\epsilon = \lambda_1/\lambda_2 - 1$.[3]
(18) Perera, S. A.; Bartlett, R. J. *J. Am. Chem. Soc.* **1996**, *118*, 7849.
(19) Muchall, H. M.; Werstiuk, N. H. *J. Phys. Chem. A* **1999**, *103*, 6599.
(20) Muchall, H. M.; Werstiuk, N. H. To be submitted.
(21) Olah, G. A.; Prakash, G. K. S.; Arvanaghi, M.; Anet, F. A. L. *J. Am. Chem. Soc.* **1982**, *104*, 7105.
(22) Yannoni, C. S.; Macho, V.; Myhre, P. C. *J. Am. Chem. Soc.* **1982**, *104*, 907.
(23) Jameson, A. K.; Jameson, C. J. *Chem. Phys. Lett.* **1987**, *134*, 461.